Effect of Sample Preparation Technique on Strain Localisation of Dense Sand under Biaxial Test Condition

Madhu Sudan Negi[1] and Mousumi Mukherjee[2*]

[1] *Research Scholar, Indian Institute of Technology, Mandi-175005, India*
[2] *Assistant Professor, Indian Institute of Technology, Mandi-175005, India*
[*]Corresponding Author, E-mail: mousumi@iitmandi.ac.in

Abstract. During the process of shearing, deformation of granular materials like dense sand is often noticed to concentrate within a narrow zone, commonly referred as shear bands. Various studies show that the formation of shear band is influenced by the internal inhomogeneity of the granular assembly. Owing to various ways of specimen generation, internal inhomogeneity arises in sample while performing laboratory experiments or carrying out micromechanics based simulations employing discrete element methods (DEM). Hence, understanding the effect of inhomogeneity, resulting from such sample generation techniques, on the formation of shear bands becomes imperative. In the present study, DEM based biaxial test simulations have been performed on the dense sand specimens, which have been prepared following two sample generation techniques. Biaxial shearing of these specimens have been conducted adopting a stress controlled flexible boundary. It has been noticed that dense specimen shows buckling and bulging type deformation accompanied with formation of localized shear bands. The initiation and propagation of persistent shear bands have been analyzed from the spatial variation of porosity and particle rotations within the specimen. The position of shear band within the specimen differs due to presence of different initial inhomogeneity within the particle packing arrangement arising due to variation in the specimen generation process.

Keywords: Discrete Element Method; Sample Generation; Biaxial Test; Flexible Boundary; Shear Band.

1 Introduction

Instabilities in geomaterials have a significant influence on the occurrence of landslides, liquefaction, and debris flows, and it often acts as a precursor to failure for geotechnical structures [1, 2]. For boundary value problems, the onset of the instability is defined as the transition from an initial homogeneous deformation field to a nonhomogeneous one. In granular assembly, e.g., dense sand, localized instability mode may arise in the form of shear band with excessive shear deformation [3, 4]. Similar to geotechnical field situations, the localized instability can also be noticed while performing different element level tests in the laboratory, such as triaxial or biaxial tests. It is to be noted that majority of the geotechnical structures, e.g., retaining walls, earthen embankments, finite and infinite slopes, and strip footing etc., conform to the plane strain condition. In these cases,

the length of the structure in one direction is significantly large resulting the strains in that direction to be negligible. In order to replicate such plane strain condition in the laboratory, biaxial tests are often employed [3-4]. During the biaxial test, further, the occurrence of localized instability has a major impact on the observed overall material response and subsequent constitutive characterization of the geomaterial [5].

Numerous laboratory tests and numerical simulations have been conducted in the past to understand the emergence and subsequent evolution of localized instability mode in sand [3–10]. It has been found that numerical studies based on discrete particle-based methods, such as DEM, can be very helpful in understanding the micromechanics of initiation and subsequent evolution of the localized instability in geomaterials [8-10]. Instability, which are identified at macro level in any element level test, are likely to initiate at the micro level due to the existence of internal heterogeneity within the specimen [8,9]. Such instability then spreads further with continued deformation and affects the shearing response of the entire assembly. The spatial distribution of internal heterogeneity within the sample may vary as a result of changes in the particle packing structure owing to the various specimen generation techniques used in DEM. Therefore, it is crucial to comprehend how these changes in heterogeneity, induced by various specimen generation techniques, affect the shearing behavior and subsequent instability response of granular assembly.

The present work incorporates two of the commonly employed specimen generation techniques in DEM, single-layered isotopic compression (IC) and multilayer undercompaction method (UCM) and investigates the influence of these specimen generation techniques on the instability response of dense sand under biaxial shearing. The initial heterogeneity within the specimens, induced by different specimen generation method, has been assessed in terms of porosity variation within the specimen. Further, the localized instability mode has been analyzed from the spatial variation of porosity and particle rotation. The influence of specimen generation techniques has also been investigated in terms of thickness and inclination of shear band.

2   DEM simulation for biaxial test

Biaxial test simulations of dense sand specimens have been conducted using DEM software, Particle Flow Code-2D, PFC2D [16]. The biaxial shearing of these specimens have been conducted adopting a stress controlled flexible boundary, and the employed micromechanical parameters along with details of model geometry are summarized in Table 1 [6]. Figure 1 shows the particle size distribution for the sand specimen, which is composed of particles in the form of circular disks, with a mean particle diameter $d_{50} = 0.993$ mm. A linear elastic contact model with Coulomb friction has been adopted to represent the normal and shear interaction between the particles.

Biaxial test simulations have been carried out in three subsequent stages, namely, Stage 1 - particle generation and compaction, Stage 2 - isotropic compression and Stage 3 - biaxial shearing. In Stage 1, the specimens have been created with an initial porosity value of $\eta = 0.178$ employing two specimen generation approaches i.e., isotopic compression (IC) and multilayer undercompaction method (UCM). In the IC method, particles are placed in an enclosed larger area ensuring no overlap and subsequently, the boundary walls are moved inward until the desired porosity or stress condition is obtained [11]. Whereas, in UCM, particles are generated in multiple layers following a

predetermined undercompaction criteria, where equal number of particles of all sizes are generated in each layer from the desired particle size distribution [12]. The UCM specimen in the present study, has been generated in four layers.

In Stage 2, isotropic compression has then been applied to each of such generated specimens for achieving a confining pressure of 200 kPa by controlling the velocity over all the boundary walls of the specimen. An interparticle friction, $\mu = 0$ has been employed during the specimen generation stages in order to generate dense specimens with extreme porosity value η_{min} at the end of Stage 2. After isotropic compression at the end of Stage 2, specimens with porosity = 0.157 and 0.158 have been generated by IC and UCM, respectively. Subsequently, in Stage 3, biaxial shearing has been performed on the generated specimens.

During the shearing stage, flexible membrane type lateral boundaries are introduced by replacing the lateral wall boundaries. Further, the specimens are compressed vertically with the strain-controlled top and bottom wall, while a constant magnitude of 200 kPa confining pressure has been maintained by applying external force [13]. The flexible membrane has been modeled with a string of uniform sized small particles of 0.1 mm diameter that are connected by strong contact bonds. An axial strain rate of 0.5 /s has been chosen in the shearing stage and the inertial number (I) corresponding to this strain rate is less than 10^{-3}, which is sufficient for ensuring the quasistatic condition [14].

Table 1. Model geometry and material parameters used for DEM simulations [6].

| Parameter	Value	Unit
Initial specimen height	100	mm
Initial specimen width	50	mm
Membrane properties		
Normal bond strength	1×10^{300}	Pa
Shear bond strength	1.5×10^{300}	Pa
Normal contact stiffness	1×10^{6}	N/m
Shear contact stiffness	1×10^{6}	N/m
Particle and wall properties		
Particle and wall friction adopted before shearing	0	-
Particle and wall friction adopted during shearing	0.5	-
Particle-wall and particle-particle normal contact stiffness	1.5×10^{8}	N/m
Particle-wall and particle-particle shear contact stiffness	1×10^{8}	N/m
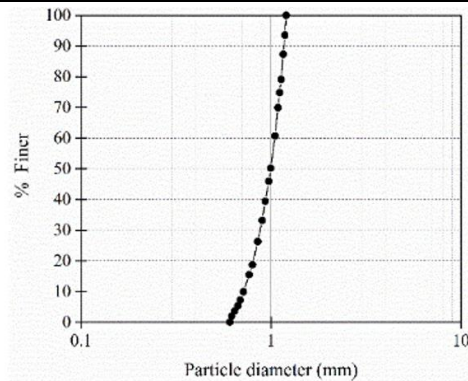
Fig. 1. Particle size distribution.

3 Influence of specimen generation technique on initial homogeneity of the specimen

3.1 Spatial variation of porosity within the specimen

The homogeneity of the specimen generated using the two specimen generation methods has been assessed in terms the variation of porosity within the specimen in both horizontal (X) and vertical (Y) directions. In this regard, the specimen has been divided into 11 number of bands in both X and Y directions as illustrated in Fig. 2(a) and (b). Porosity in the ith band (η^i) has been estimated based on eqn. (1). Additionally, standard deviation in the estimated band porosities, S_k^{η} has been also calculated using eqn. (2) and is used for assessing the homogeneity of specimen.

$$\eta^i{}_k = 1 - \frac{A_i^p}{A_i^b} \tag{1}$$

$$S_k^{\eta} = \sqrt{\frac{1}{m-1}\sum_{i=1}^{m}\left(\eta^i{}_k - \bar{\eta}\right)^2} \tag{2}$$

A_i^p is the total area of the particles inside the band, A_i^b is the band area, $\bar{\eta}$ is the average porosity for the specimen, m is the total number of bands and k denotes the direction, i.e., X or Y.

Figure 2(c) depicts the histograms of S_k^{η} in the X and Y directions at the end of Stage 1 and Stage 2 for both the specimens. The variation of individual band porosity has also been presented in Figure 3 for both the specimens. The estimated values of S_k^{η} for these specimens, as depicted in Fig. 2(c) at the end of Stage 1, clearly indicates that there exists some level of heterogeneity within specimens. The specimen generated by IC technique exhibits highest magnitude of S_k^{η} at the end of Stage 1. Since in the Stage 1 of IC method, forces are applied through all the four boundary walls, the particles slide along the wall boundaries and results into formation of region with high porosity near the central part of the specimen. This can also be observed from Fig. 3(a) and (b), which shows high porosity in the central bands in both X and Y directions for the specimen generated with IC method.

Further, it can be noticed from Fig. 2(c) that specimen generated employing UCM also exhibits high heterogeneity at the end of Stage 1. This is attributed to the initial undercompaction of the bottom layer adopted in the UCM technique, which creates regions with large porosity in the lower layers of the specimen at the end of Stage 1 as evident from Fig. 3(b). The heterogeneity in both the specimens reduces significantly after the isotropic compression exerted in Stage 2, which can be observed from Fig. 2(c) with the decrease in the magnitude of S_k^{η}. This might be a result of the particle rearrangement that occurs in Stage 2 to transfer the higher contact forces for achieving the desired confining pressure.
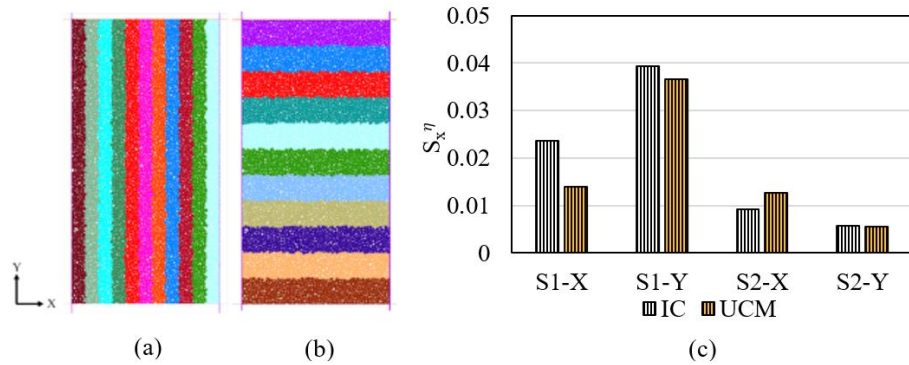
Fig. 2. Bands to compute spatial variation of porosity in (a) X direction (b) Y direction; (c) variation of standard deviation in band porosity, S_k^η for specimens generated employing IC and UCM techniques at the end of Stage 1 (S1) and Stage 2 (S2) in X direction and Y direction.
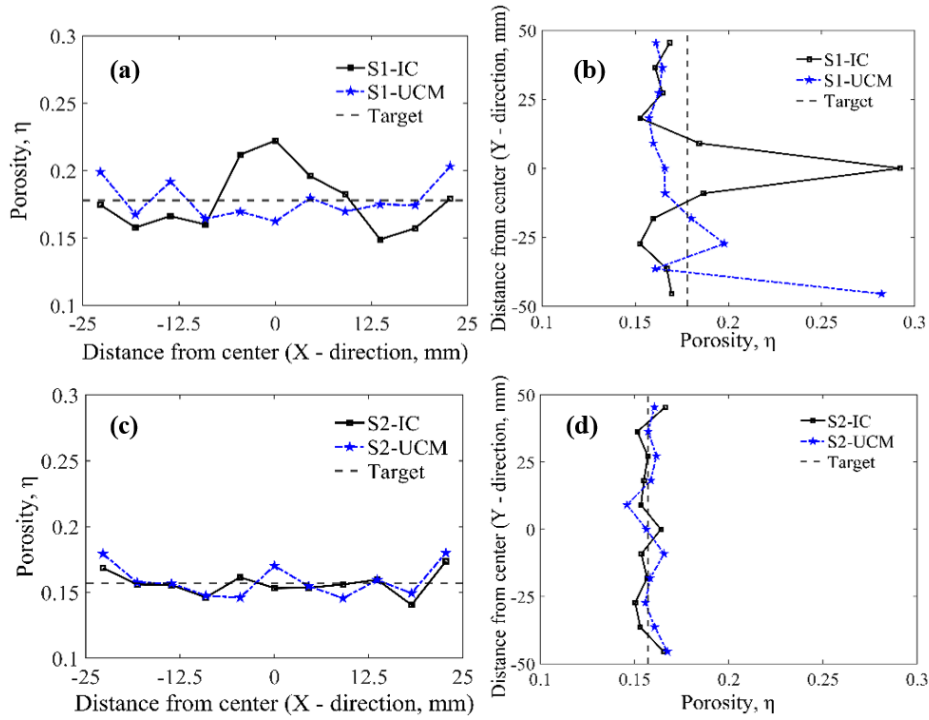

Fig. 3. Variation of band porosity, η in the specimens generated employing IC and UCM techniques at the end of Stage 1 and Stage 2 in (a, c) X direction and (b, d) Y direction, respectively.

4   Macro level response of the specimen during biaxial shearing

Biaxial shearing has been performed in the Stage 3 on both the dense specimens generated using IC and UCM techniques. The stresses and strains have been estimated from the average value of three representative area elements (RAE) that has been placed within the specimen [6]. To obtain precise estimate of stresses and strains, RAE have

been considered to evolve with the continued deformation process maintaining a constant (95%) area coverage in reference to the deformed configuration of the specimen [17].

Figure 4 presents the macro level stress-strain and volumetric response of the specimens. Both the specimens show typical stress-strain and volumetric response of dense specimen as commonly observed in the laboratory tests. As shown in Fig. 4(a), for both the specimens, the stress deviator initially increases with increasing axial strain to a peak value and then decreases exhibiting strain-softening behavior reaching to a similar stress state at larger strain level. The volumetric strain decreases at first showing an initial compression till 0.4 % axial strain level and then increases continuously corresponding to dilation with increasing axial strain (Fig. 4b). It can also be observed that, the specimens show identical volumetric responses up to 3% axial strain, after that, variations in the volumetric behavior can be observed due to the formation of localized instabilities, e.g., shear bands, within the specimen.
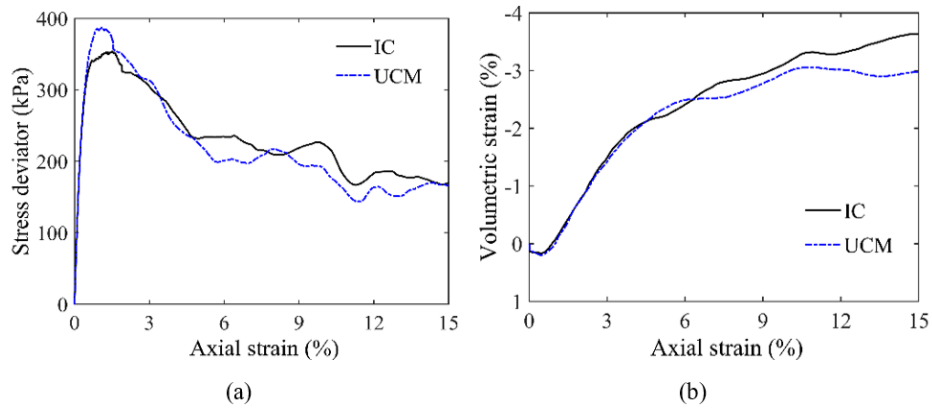

Fig. 4. Evolution of (a) stress-strain and (b) volumetric response.

5 Micro level response of the specimens during biaxial shearing

5.1 Local porosity variation within the specimens

In order to calculate the porosity field, several small RAE's have been employed in the specimen keeping the ratio of diameter of RAE to the average particle diameter (d_{50}) as 6.50 [17]. Figure 5(a) and (b) presents the spatial variation of the porosity at three different strain levels for both the specimens. Several loosely packed regions with high porosity spatially distributed within the specimen can be observed at the initial state. This local density variation in both the specimens is due to the variation in particle packing arrangement occurring from different sample generation methods. As the axial strain increases, several zones dilate concentrating around the initial loose-packed regions forming several potential shear bands. With further shearing, these zones connect with each other and enlarge to form the persistent shear bands with increased thickness at large strain levels. It is to be noted that both the specimens form two conjugate shear bands; however, the position of the shear band for both the specimens differ corresponding to the initial location of high porosity regions.

5.2 Accumulated particle rotation within the specimens

Particle rotation is a major micro level mechanism, which affects the mechanical behavior of the granular materials [15]. Figure 5(c) and (d) depicts the spatial variation of accumulated particle rotations within both the specimens at three different strain levels. It has been observed that excessive particle rotations occur within the cross-type band region well after the peak stress and it continues to increase with further shearing. This cross-type region with high rotation has been identified as the shear band and the position of which is the same as the location of high porosity region. The left and right bands exhibits clockwise (negative) and anticlockwise (positive) rotations, respectively due to the displacement field produced by the applied biaxial loading conditions. As observed from the porosity field, the position of shear bands corresponding to the particle rotation differs in the two specimens owing to the different initial heterogeneity within the specimen.
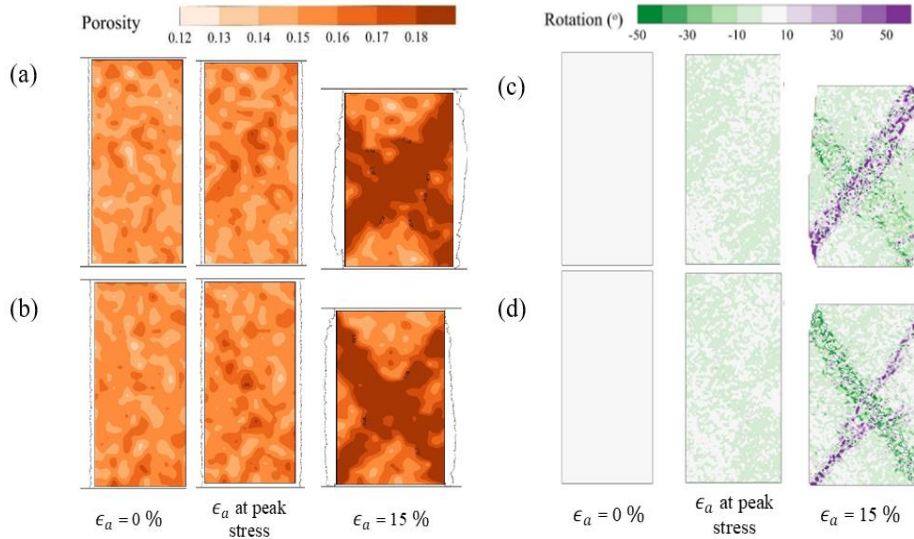

Fig. 5. (a, b) Spatial variation of porosity and (c, d) accumulated rotation at various global axial strain levels, ϵ_a for specimens generated by IC and UCM, respectively.

5.3 Inclination and thickness of shear band

The characteristics of the shear band such as the thickness and inclination can be obtained from the variation of porosity and particle rotations within the specimen [6,10,15]. In the present study, the inclination and thickness of the shear band has been calculated at 15 % axial strain level, i.e., the strain level where persistent shear bands have been noticed to develop. Since a cross-type shear band develops in all the specimens, the inclination has been calculated for both the left and right bands, and the average of these two values has been reported as the final inclination.

The histogram in Fig. 6(a) summarizes the estimated band inclination angle corresponding to porosity and accumulated particle rotations. It has been observed that porosity based estimation indicates a higher value of shear band inclination in comparison

to the rotation based predictions. The shear band inclination varies in the range of 52° - 57° for both specimens due to initial heterogeneity in the particle packing arrangement induced by different specimen generation process.

In order to calculate the band thickness, the cross-type shear bands have been divided into four parts. In each of these parts, straight profiles have been established and the distance of the profile exhibiting porosity and rotation higher than the specimen average has been considered as the thickness of the shear band [6]. Similar to the band inclination, the thickness of the shear band also varies for both specimens as depicted in Fig. 6(b). The band thickness varies in the range of 7-14 times of d_{50}. It can be also noticed that the band thickness corresponding to porosity gives a higher value as compared to accumulated rotation based estimation.
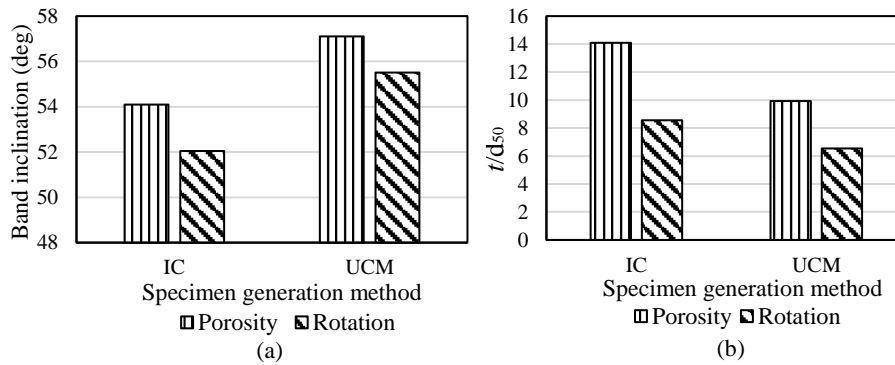

Fig. 6. (a) Inclination and (b) thickness (t/d_{50}) of shear band obtained in specimens generated by IC and UCM.

6   Conclusion

In the current work, two different specimen generation techniques employed in DEM have been analyzed with focus on the initial sample heterogeneity and their effects on the localized instability mode of dense specimen during the biaxial shearing process. The following conclusions have been drawn based on the findings of the DEM analysis:

- At the end of the particle generation phase, i.e., Stage 1, specimens exhibit maximum heterogeneity due to enhanced particle sliding. However, at the end of isotropic compression phase, i.e., Stage 2, relatively homogeneous specimens are generated by both the methods.
- Specimens generated by these two techniques exhibit similar stress-strain responses; whereas, significant variations can be noticed in the volumetric responses after an axial strain level of 3 % due to the occurrence of localized instability in form of shear bands within the specimens.
- The position, inclination and thickness of the shear band varies for both the specimens owing to different particle packing arrangements generated by various specimen generation techniques.
- Porosity based estimation of thickness and inclination of shear band predicts higher value as compared to the accumulated particle rotation based estimate.

Acknowledgement

References

1. Olson, S.M., Stark, T.D., Walton, W.H., Castro, G.: 1907 Static Liquefaction Flow Failure of the North Dike of Wachusett Dam. Journal of Geotechnical and Geoenvironmental Engineering. 126, 1184–1193 (2000).
2. Widuliński, L., Tejchman, J., Kozicki, J., Leśniewska, D.: Discrete simulations of shear zone patterning in sand in earth pressure problems of a retaining wall. International Journal of Solids and Structures. 48, 1191–1209 (2011).
3. Vardoulakis, I.: Shear band inclination and shear modulus of sand in biaxial tests. International Journal for Numerical and Analytical Methods in Geomechanics. 4, 103–119 (1980).
4. Han, C., Drescher, A.: Shear bands in biaxial tests on dry coarse sand. Soils and Foundations. 33, 118–132 (1993).
5. Andrade, J.E., Borja, R.I.: Modeling deformation banding in dense and loose fluid-saturated sands. Finite Elements in Analysis and Design. 43, 361–383 (2007).
6. Tian, J., Liu, E., He, C.: Shear band analysis of granular materials considering effects of particle shape. Acta Mechanica. 231, 4445–4461 (2020).
7. Peters, J.F., Walizer, L.E.: Patterned Nonaffine Motion in Granular Media. Journal of Engineering Mechanics. 139, 1479–1490 (2013).
8. Darve, F., Servant, G., Laouafa, F., Khoa, H.D.V.: Failure in geomaterials: Continuous and discrete analyses. Computer Methods in Applied Mechanics and Engineering. 193, 3057–3085 (2004).
9. Hadda, N., Nicot, F., Bourrier, F., Sibille, L., Radjai, F., Darve, F.: Micromechanical analysis of second order work in granular media. Granular Matter. 15, 221–235 (2013).
10. Lü, X., Zeng, S., Li, L., Qian, J., Huang, M.: Two-dimensional discrete element simulation of the mechanical behavior and strain localization of anisotropic dense sands. Granular Matter. 21, 1–16 (2019).
11. Potyondy, D.O., Cundall, P.A.: A bonded-particle model for rock. International Journal of Rock Mechanics and Mining Sciences. 41, 1329–1364 (2004).
12. Jiang, M.J., Konrad, J.M., Leroueil, S.: An efficient technique for generating homogeneous specimens for DEM studies. Computers and Geotechnics. 30, 579–597 (2003).
13. Wang, Y.H., Leung, S.C.: A particulate-scale investigation of cemented sand behavior. Canadian Geotechnical Journal. 45, 29–44 (2008).
14. Midi, G.D.R.: On dense granular flows. European Physical Journal E. 14, 341–365 (2004).
15. Bardet, J.P.: Observations on the effects of particle rotations on the failure of idealized granular materials. Mechanics of Materials. 18, 159–182 (1994).
16. Itasca Consulting Group, Inc. PFC-Particle Flow Code, Ver. 5.0. (2014), Minneapolis.
17. Negi, M. and Mukherjee, M. Assessment of macro and micro level heterogeneities for characterizing mechanical behavior of sand in biaxial test employing DEM, 15th World Congress on Computational Mechanics and 8th Asian Pacific Congress on Computational Mechanics WCCM-APCOM (2022), Yokohama, Japan.